Understanding Ligninase-Mediated Reactions of Endocrine Disrupting Chemicals in Water: Reaction Rates and Quantitative Structure-Activity Relationships

Liang Mao, Lisa M. Colosi, Shixiang Gao*, Qingguo Huang*

1 table, 7 figures, 10 pages total

I. Supporting Data and Figures.

TABLE S1. Substrate parameters used in QSAR relationships for LiP reactivity.

Compound	$\ln(k_{CAT})$ (s^{-1})	E_{HOMO} (eV)	E_{LUMO} (eV)	E_{LUMO}-E_{HOMO} (eV)	Volume (Å^3)
E1	1.45	-5.77	7.64	13.41	264
E2	0.21	-6.98	7.83	14.81	268
E3	1.73	-7.14	7.74	14.88	275
EE2	1.86	-7.12	7.77	14.89	292
NP	2.04	-7.24	7.94	15.18	242
BPA	5.35	-6.95	7.79	14.74	222

[a] Molecular descriptors are abbreviated as follows: energy of the highest molecular orbital (E_{HOMO}), energy of the lowest unoccupied molecular orbital (E_{LUMO}).

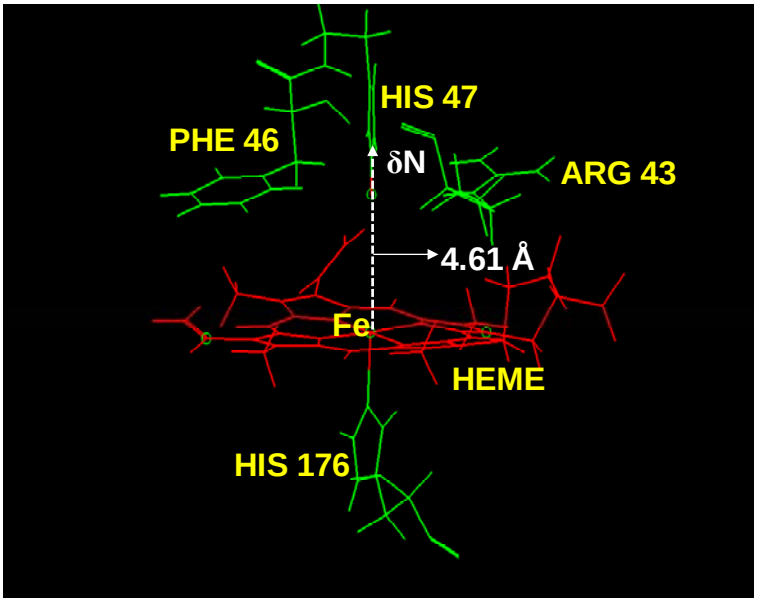

FIGURE S1. Stereo view of the catalytic cavity in LiP. LiP structure was downloaded from RCSB protein data bank (www.rcsb.org/pdb) (ID 1B82) and viewed by HyperChem Molecular Modeling System. All residues were removed except for those shown, which were believed to form the heme binding pocket (ref 16 in the paper).

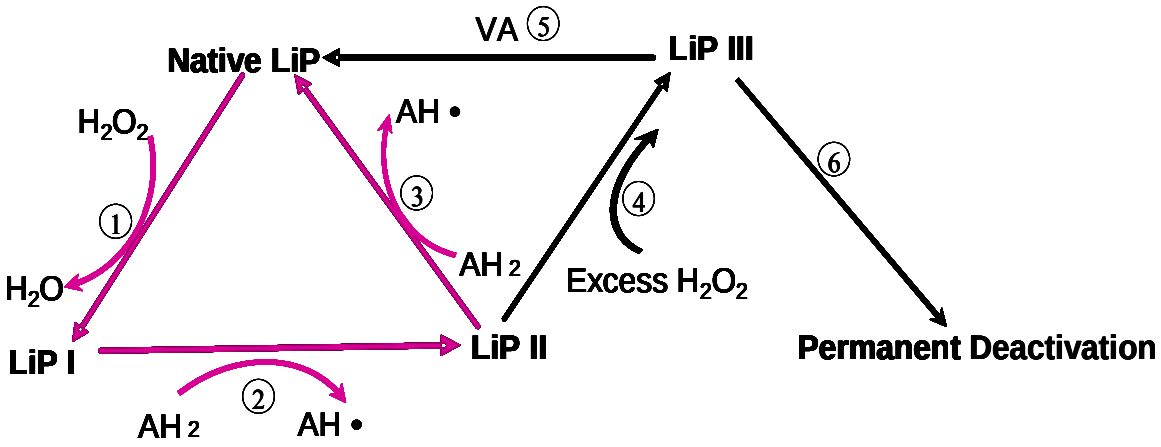

FIGURE S2. Schematic depiction of LiP catalytic process. The arrows in pink color represent the three-step catalytic cycle and those in black denote LiP inactivation via LiPIII and its mitigation in the presence of VA.

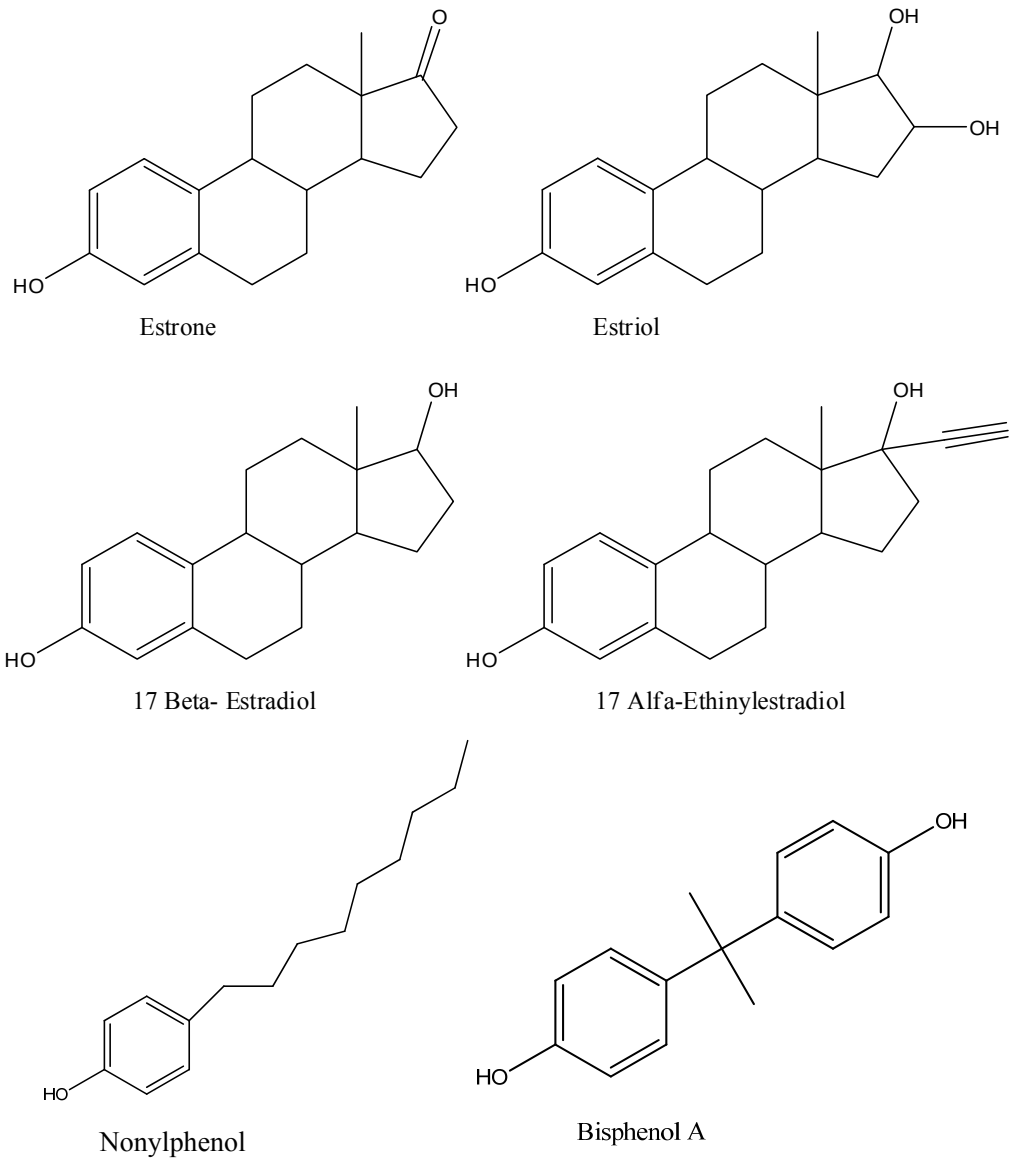

FIGURE S3. Molecular structures of selected estrogens.

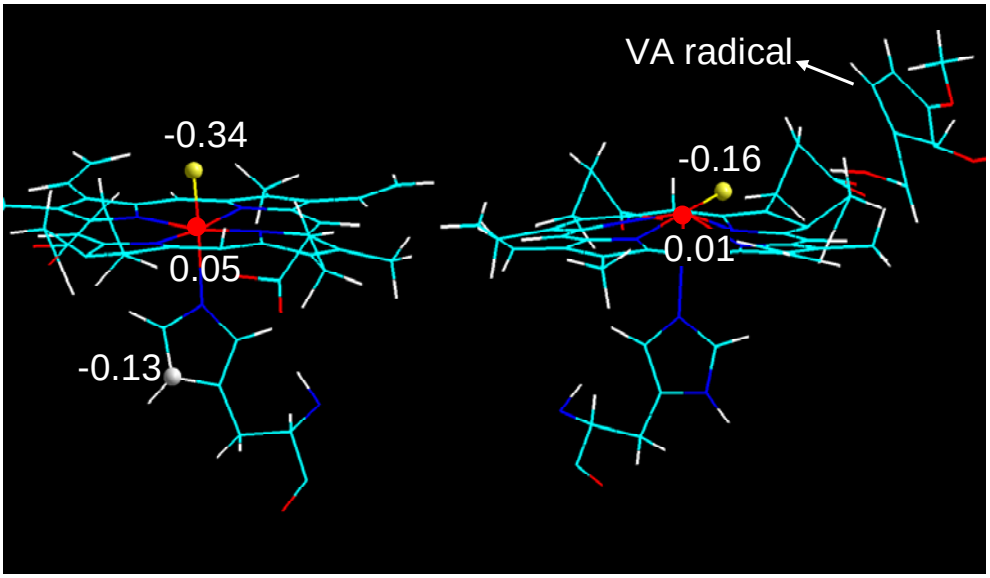

FIGURE S4. Charge distribution of the selected subset in the enzyme intermediates. The left is LiPII and the right is the LiPII-VA$^{\bullet+}$ complex.

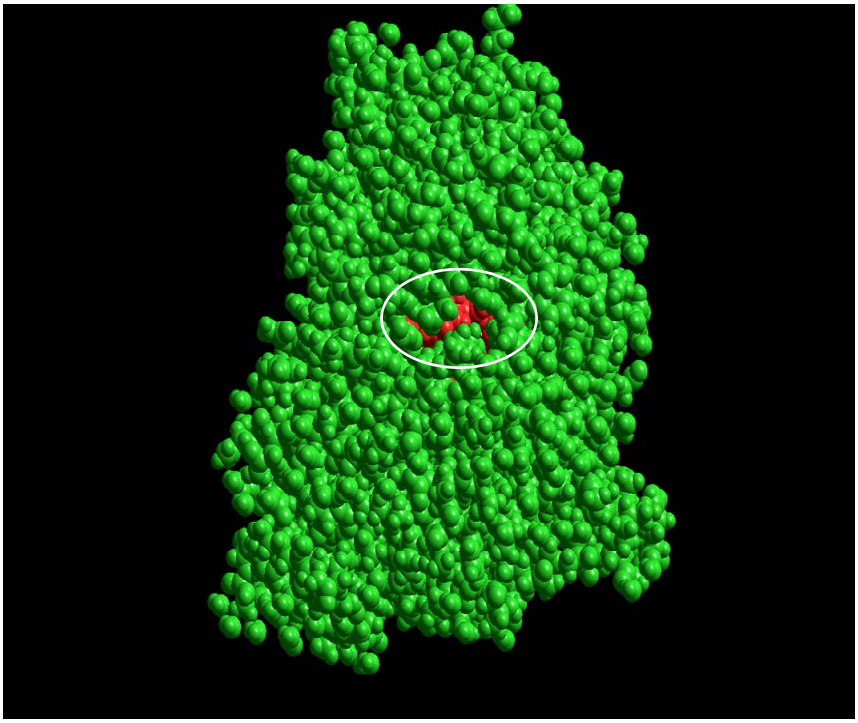

FIGURE S5. Stereo view of the open channel that connects heme pocket to LiP surface. The heme (red) is buried inside the protein, and the circle indicates the small opening connecting the active site with outside of the protein.

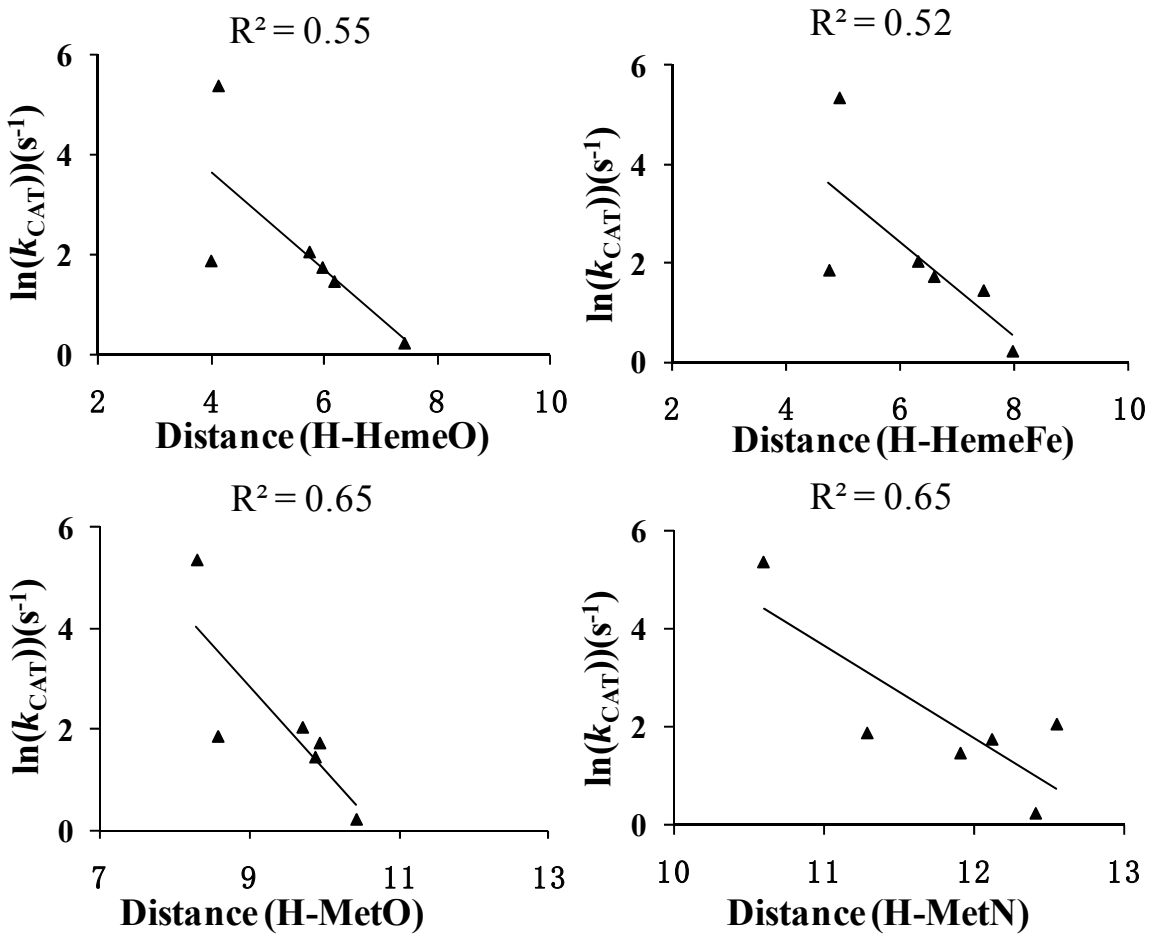

FIGURE S6. Correlations between ln(k_{CAT}) and simulation-estimated average binding distances (Å). Distances are relative to the substrate's phenolic proton, as measured from four locations in the enzyme's catalytic pocket: 1) the heme-bound oxygen (H-HemeO), as shown at upper left; the heme iron (H-HemeFe), as shown at upper right; the oxygen of MET172 (H-MetO), as shown at lower left; and the nitrogen of MET172 (H-MetN), as shown at lower right. These distances were obtained through molecular simulations of enzyme/substrate complexes comprising LiP II.

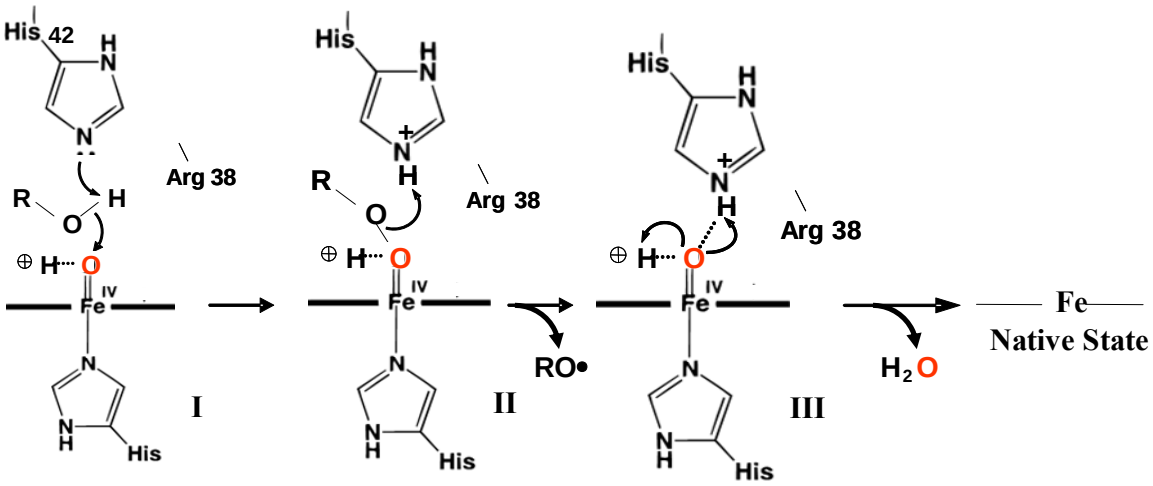

FIGURE S7. Schematic representation of the HRP-catalyzed EDCs reaction cycle, (ref 33, 35 in the paper). I, a hypothetical HRPII-substrate complex with substrate (ROH) bound as an electron donor. II-III, the transition states. The RO-H bond is undergoing heterolytic bond cleavage and H^+ is temporally stabilized by the δN in HIS42's imidazole ring and then transferred to the heme-bound oxygen. Amino acid residues in the active site (His-42, His-172 and Arg-38 in HRP) are shown.

II. Additional Description of Selected Experimental Procedures

HPLC Analysis. A Shimadzu LC 20TA High Performance Liquid Chromatograph (HPLC) equipped with a RF-10A fluorescence detector was used to quantify the hormones. The separation was performed on an Ascentic C18 reverse phase column (250 × 4 mm, 5 μm particle, Supelco). Injection volume was 5 μL, and the excitation and emission wavelengths were 280 and 312 nm, respectively, for the fluorescence detector. The mobile phase was made up of ACN and water and eluted at 1 mL/min using the following gradient program: 0-10min, changing from 40/60% to 60/40% ACN/DDI; 10-25min, changing from 60/40% to 80/20% ACN/DDI. Experiments were conducted for all four estrogens in the presence and absence of VA, but the data for reaction of E1 in the presence of VA was not obtained because an impurity in VA interfered with HPLC detection of E1.

Optimization of Simulation Model for LiP II-VA$^{\bullet+}$ Complex. VA$^{\bullet+}$ was placed at a random location within the small opening on LiP indicated Figure S5 and then subjected to an series of optimizations to achieve a LiP II-VA$^{\bullet+}$ complex model. The OPLS molecular mechanics force field was utilized in a 1000-step Monte Carlo (MC) simulation during which all model components were held fixed in place except for the VA$^{\bullet+}$ and the three distal residues known critical in docking, ARG43, PHE46 and HIS47. This and all subsequent MC simulations were performed in vacuo at 300 K. In each step, a randomly selected atom was moved a random distance (< 0.05 Å) in a random direction. Moves resulting in negative energy changes were selected. Moves resulting in positive energy changes were accepted with a probability defined by Boltzmann distribution, $f(x) = e^{-\Delta E/K_B T}$ where ΔE is the magnitude of the energy increase, K_B is the Boltzmann constant, and T is

absolute temperature (*29*). Following completion of the first 1000-step MC simulation, the lowest energy conformation of $VA^{\bullet+}$ was recalled and its geometry was optimized using OPLS and Polak-Ribiere. The resultant optimized geometry was then used as the starting configuration for the next 1000-step MC simulation in which the $VA^{\bullet+}$, ARG43, PHE46 and HIS47 were once again allowed to move freely. This process, MC simulations alternating with OPLS optimizations of the $VA^{\bullet+}$ alone, was iterated until the energy decrease between two consecutive geometry-optimized structures was less than 1 kcal/mol. The final conformation with the lowest energy was taken as the computational model of LiP II-$VA^{\bullet+}$ complex. Prior to using the LiP II-$VA^{\bullet+}$ model in molecular simulations, charge distribution was reassigned for the subset structure that comprises $VA^{\bullet+}$, the heme iron and its associated oxygen. The ZINDO/1 UHF method was again used to assign charges on this subset structure and the multiplicity was set to quartet to reflect the two unpaired electrons of the Fe=O and one unpaired electrons of the $VA^{\bullet+}$ (*25*). The calculated net charges on the heme iron (+0.01) and the heme-bound oxygen (-0.16) are shown in Figure S4 (right).